Colloids and Surfaces B: Biointerfaces 84 (2011) 354–359

Contents lists available at ScienceDirect

Colloids and Surfaces B: Biointerfaces

journal homepage: www.elsevier.com/locate/colsurfb

Attachment of *Pseudomonas putida* onto differently structured kaolinite minerals: A combined ATR-FTIR and ^{1}H NMR study

Ioanna A. Vasiliadou[a,*], Dimitris Papoulis[b], Constantinos V. Chrysikopoulos[a], Dionisios Panagiotaras[c], Eleni Karakosta[d], Michael Fardis[d], Georgios Papavassiliou[d]

[a] *Environmental Engineering Laboratory, Civil Engineering Department, University of Patras, 26500 Patras, Greece*
[b] *Department of Geology, University of Patras, 26500 Patras, Greece*
[c] *Department of Mechanical Engineering, Technological Educational Institute (TEI) of Patras, 26334 Patras, Greece*
[d] *Institute of Materials Science, NCSR Demokritos, 15310 Aghia Paraskevi, Attiki, Greece*

ARTICLE INFO

Article history:
Received 24 July 2010
Received in revised form 15 January 2011
Accepted 20 January 2011
Available online 26 January 2011

Keywords:
Pseudomonas putida
Kaolinite
Isotherms
ATR-FTIR spectroscopy
Nuclear Magnetic Resonance

ABSTRACT

The attachment of *Pseudomonas* (*P.*) *putida* onto well (KGa-1) and poorly (KGa-2) crystallized kaolinite was investigated in this study. Batch experiments were carried out to determine the attachment isotherms of *P. putida* onto both types of kaolinite particles. The attachment process of *P. putida* onto KGa-1 and KGa-2 was adequately described by a Langmuir isotherm. Attenuated Total Reflection Fourier Transform Infrared Spectroscopy and Nuclear Magnetic Resonance were employed to study the attachment mechanisms of *P. putida*. Experimental results indicated that KGa-2 presented higher affinity and attachment capacity than KGa-1. It was shown that electrostatic interactions and clay mineral structural disorders can influence the attachment capacity of clay mineral particles.

1. Introduction

Typical soils are very complex and heterogeneous systems because they are composed of various mineral particles, organic matter, metal oxides and microorganisms [1]. Natural colloids are present in the subsurface or formed in situ through geochemical alteration of primary minerals [2]. Clay minerals (hydrous aluminosilicates) are considered excellent adsorbent materials because they are the finest inorganic component in soils and sediments with high specific surface area, high cation exchange capacity, chemical stability and layered structure [3]. Thus, the sorption of pollutants such as metal ions [3,4], viruses [5,6], pesticides [1,7] and other chemicals [8] onto clay minerals has been extensively studied both experimentally and theoretically.

The presence of bio-colloids (e.g. bacteria and viruses) in the subsurface and groundwater could be attributed to the release of particles from septic tanks, broken sewer lines or from artificial recharge with treated municipal wastewater [9–11]. Bio-colloid transport in the subsurface is significantly affected by attachment onto the solid matrix [12–15]. Bio-colloid attachment onto mobile or suspended in the aqueous phase soil particles (e.g. clay or other minerals) may also influence bio-colloid fate and transport in porous media [16–19].

The transport of bacteria in the subsurface environment may be inhibited by attachment onto mineral surfaces or clay particles [18,20]. Foppen and Schijven [21] and Kim et al. [22] reported that the attachment of *Escherichia coli* onto goethite-coated sand increased as the coated sand content increased. Dhand et al. [18] showed that the retention of *Mycobacterium avium* subsp. *paratuberculosis* was higher in clay soil columns than sandy-soil columns. Leon-Morales et al. [23] observed that the presence of laponite influenced the detachment of *Pseudomonas* (*P.*) *aeruginosa* SG81 biofilm from quartz sand. Recently, Vasiliadou and Chrysikopoulos [24] reported that kaolinite colloidal particles hindered the migration of *P. putida* in columns packed with glass beads.

Clay minerals have been reported to affect the growth and metabolic activity of microorganisms. Rong et al. [25] reported that kaolinite and montmorillonite enhanced the exponential growth of *Bacillus thuringiensis*. Courvoisier and Dukan [26] indicated that the degradation rate of glucose was reduced, while the growth of *E. coli* was increased, due to the presence of kaolinite. Also, clay minerals may have a positive impact on the degree of bacterial-mediated hydrocarbon [27], oil [28] or pesticides [1] breakdown, may support bacterial growth [29], and can alter the survival time of bacteria [30]. Therefore, bacterial attachment onto clay

* Corresponding author. Tel.: +30 2610 996 528; fax: +30 2610 996 573.
E-mail addresses: ivasiliadou@upatras.gr, vasiliadou.ioanna@gmail.com (I.A. Vasiliadou).

0927-7765/$ – see front matter © 2011 Elsevier B.V. All rights reserved.
doi:10.1016/j.colsurfb.2011.01.026

particles is quite important and has received considerable attention.

The factors affecting bacterial attachment onto minerals, such as pH, ionic strength and temperature have been investigated by many scientists. Yee et al. [31] indicated that *Bacillus* (*B.*) *subtilis* displayed a higher affinity for corundum surfaces than for quartz surfaces, and that bacterial attachment onto corundum increased as the pH and ionic strength decreased. Shashikala and Raichur [32] reported that *B. polymyxa* attachment onto hematite was higher than attachment onto quartz, because hematite was more hydrophobic. Jiang et al. [33] showed that the adhesion of *P. putida* onto kaolinite, goethite and montmorillonite decreased gradually in the pH range 3–10, while electrostatic forces were considered to play the most important role. Rong et al. [34] observed that larger amounts of *P. putida* were attached onto kaolinite than montmorillonite and suggested that the bacterial attachment onto clay minerals occurred due to the existence of non-electrostatic forces (hydrogen bonding, van der Waals force, and hydrophobic interactions).

Attachment of bacteria onto minerals can also be affected by the cell wall structure (physiological state) of the bacteria. Grasso et al. [35] indicated that the physiological state of *P. aeruginosa Olin* affected its surface thermodynamic characteristics and its adhesion to dolomite. The *B. subtilis* (Gram-positive bacterium) was observed to attach more than *P. mendocina* (Gram-negative bacterium) onto Fe-coated quartz surfaces [36]. Although a number of studies focused on the factors affecting the attachment of bacteria onto minerals, the precise attachment mechanisms are not fully understood.

The objective of the present study was to examine how the attachment of *P. putida* onto clays is affected by the clay mineral structure. Equilibrium attachment experiments were conducted by using two structurally different kaolinites (well and poorly crystallized kaolinite). The interactions and binding mechanism between *P. putida* and kaolinites were evaluated using Attenuated Total Reflection Fourier Transform Infrared Spectroscopy (ATR-FTIR) and Nuclear Magnetic Resonance (NMR).

2. Materials and methods

2.1. Bacteria and culture preparation

The *P. putida* (ATCC17453) cells were initially cultured in 10 ml of nutrient broth (Laury Pepto Bios Broth 35.6 g l^{-1}, Biolife), over a period of 20 h and incubated at 30 °C in an orbital shaker (140 rpm), until an optical density at 600 nm (OD_{600}) of 0.5 was reached. Subsequently, 5 ml of culture was transferred to 250 ml of the same medium and incubated at 30 °C for 20 h.

Cells in the late exponential growth phase (OD_{600} = 0.9) were harvested by centrifugation (10 min at $3000 \times g$) and washed three times with distilled deionized water (ddH_2O). Harvesting at the end of the logarithmic phase minimizes the potential for cell numbers increase during the attachment experiments. After the washing procedure, bacteria were diluted in ddH_2O to obtain the desired experimental concentration of 1.76×10^6 to 1.54×10^9 CFU ml^{-1}, with a dry biomass concentration in the range of 10–1842 mg bacteria l^{-1}. Following the work by Rong et al. [34], the optical density of bacteria in ddH_2O was analyzed at a wavelength of 410 nm by a UV–vis spectrophotometer (UV-1100, Hitachi). The concentration of bacterial cells was calibrated with a standard curve of bacterial optical density.

The Zeta potential of the bacterial suspension in ddH_2O (pH = 7) was determined to be -44.16 ± 1.6 mV using a Zeta potential analyzer (ZetaSizer, Malvern Instruments Corporation). The isoelectric point (IEP), which is the pH where the electrophoretic mobility changes from positive to negative, was measured by acid–base potentiometric titration and Zeta potential analyzer, and it was found to be pH_{IEP} = 2.1. The equivalent spherical diameter of *P. putida*, which is a rod-shaped bacterium, was estimated to be 2.16 ± 0.44 μm.

2.2. Minerals

KGa-1 (low-defect, well crystallized, from Washington County, Georgia USA) and KGa-2 (high-defect, poorly crystallized, from Washington County, Georgia USA) kaolinites were purchased from Clay Minerals Society (USA). Both mineral suspensions were prepared using the same procedure. Specifically, 50 g of the clays (KGa-1 or KGa-2) was mixed with 100 ml of ddH_2O in a 2 l beaker, followed by the addition of an adequate amount of hydrogen peroxide (30% solution) to oxidize organic matter. The mineral suspension was adjusted to pH = 10 using 0.1 M NaOH. The suspension was diluted to 2 l and the <2 μm clay fraction was separated by sedimentation. The separated clay suspension was flocculated by adding 0.5 M $CaCl_2$ solution. The clay particles were washed with ddH_2O and ethanol, and dried at 60 °C, as recommended by Rong et al. [34].

The particle size of the KGa-1 clay fraction (treated sample) ranged between 0.396 and 1.718 μm, while the particle size of the KGa-2 clay fraction (treated sample) ranged between 0.459 and 1.484 μm. The Specific Surface Area (SSA) of KGa-1 and KGa-2 standard mineral samples (untreated) as given by the Clay Minerals Society was 10.05 ± 0.02 and 23.50 ± 0.06 m^2 g^{-1}, respectively, while the cation exchange capacity (CEC) was 2.0 and 3.3 mequiv./100 g, respectively. The Zeta potentials of KGa-1 and KGa-2 suspensions (clay fraction-treated) at pH = 7 in ddH_2O were estimated to be -22.53 ± 2.11 and -16.50 ± 0.35 mV, respectively. The IEP for KGa-1 and KGa-2 was estimated to be pH_{IEP} = 2.5 and pH_{IEP} = 2.9, respectively.

2.3. Attachment of bacteria onto minerals

Batch experiments were performed in order to measure the attachment of *P. putida* onto KGa-1 and KGa-2 as a function of bacterial concentration. One hundred and seventy milligrams (170 mg) of minerals were mixed with 10 ml *P. putida* ddH_2O solution containing a concentration of bacteria in the range of 10–1840 mg of *P. putida* l^{-1}. The mixture was adjusted to pH = 7 by adding appropriate amounts of 0.1 M NaOH and 0.1 M HNO_3 solution and was gently shaken at 26 ± 1 °C for 120 min. Subsequently, 1.5 ml of Histodenz solution (60% by weight, Sigma D2158) was injected into the suspension [33] and the mixture was centrifuged at $2500 \times g$ for 4 min. Histodenz was used as a density gradient separation reagent in order to separate the suspended bacteria from those sorbed onto kaolinite particles because the size of bacteria (2.16 μm) and kaolinite (<2 μm) particles was of the same order.

The suspension of unattached bacteria in the supernatant was pipetted out and measured directly by spectrophotometry at 410 nm. The percentage of attached bacteria was determined by subtracting the mass of bacteria that remained in suspension from the initial mass of bacteria. The experimental data indicated that equilibrium was reached at approximately 60–80 min. Therefore, a contact time of 2 h was chosen for the equilibrium experiments, which were performed in triplicates to ensure reproducibility.

It should be noted that Histodenz is a nonionic iodinated gradient medium, which readily dissolves in water to give nontoxic, autoclavable solutions. Histodenz should be avoided if the analysis involves spectrophotometric measurements in the ultraviolet range, because the absorption spectrum shows a maximum at 244 nm [37]. To assess whether Histodenz interfered with bacteria measurements, the absorbance of standard bacteria samples was measured at 410 nm. It was observed that Histodenz did not affect the linearity of the standard curve.

2.4. X-ray diffraction (XRD)

The mineralogical composition of KGa-1 and KGa-2 standard mineral samples, their clay fractions (treated), and bacteria–clay complexes from the attachment experiments were determined by XRD using a Bruker D8 advance diffractometer, with Ni-filtered CuKα radiation. XRD patterns were obtained from random powder, oriented samples and clay fractions at a 2θ range from 2° to 60°, scanned at 2° min^{-1}. Random powder mounts were prepared for selected samples by gently pressing the powder into the cavity holder. Oriented clay powder samples were prepared by the dropper method. The samples were fractionated to <2 μm by gravity sedimentation.

2.5. Attenuated Total Reflection-Fourier Transform Infrared Resonance Spectroscopy (ATR-FTIR)

ATR-FTIR measurements were recorded using ATR MIRacle accessory of PIKE technologies (diamond crystal) attached to the EQUINOX 55 FT-IR spectrometer (BRUKER). ATR-FTIR spectroscopy was selected because it is a suitable technique for the characterization of materials, which are either too thick or too strong absorbing to be analyzed by transmission spectroscopy. The method does not require any special sample preparation.

2.6. Nuclear Magnetic Resonance (NMR)

^{1}H pulsed NMR experiments were performed on *P. putida* sorbed onto both KGa-1 and KGa-2, using a modified Bruker NMR spectrometer. All measurements were carried out at room temperature, in a lightweight permanent Halbach magnet with a very low static magnetic field B_0 = 0.29 T, corresponding to proton resonance frequency of $\omega_0/2\pi$ = 12.17 MHz, following the procedure outlined by Karakosta et al. [38].

The spin–lattice relaxation time (T_1) of all samples was measured using a standard saturation recovery technique $[(\pi/2)-t-(\pi/2)-\tau-(\pi)]$ with interpulse delay (t) ranging from 1 ms to 6 s. The signal was detected by the common Hahn echo pulse sequence. Analysis was performed by using the inverse Laplace transform, which lead to the T_1 distribution profiles [39]. The numerical Laplace inversion of the ^{1}H NMR saturation recovery curves was obtained by using a modified CONTIN algorithm, introduced by Provencher [40], which was adapted on a Matlab application.

3. Results and discussion

3.1. Equilibrium attachment of P. putida

The batch equilibrium experimental data are shown in Fig. 1, and they are fitted with a Langmuir type isotherm [33,34]:

$$C_{bc} = \frac{Q^{\circ}\alpha_1 C_{b_{eq}}}{1+\alpha_1 C_{b_{eq}}} \quad (1)$$

where C_{bc} ((mg bacteria)(g clay)$^{-1}$) is the bacteria concentration attached onto clay particles, Q° ((mg bacteria)(g clay)$^{-1}$) is the maximum amount of bacteria that may be attached onto clay particles, α_1 ((l)(mg bacteria)$^{-1}$) is the constant related to the attachment energy, and $C_{b_{eq}}$ ((mg bacteria)(l)$^{-1}$) is the concentration of bacteria at equilibrium. The fitted parameters for the two clays examined are listed in Table 1.

The experimental data indicated that more *P. putida* were attached onto KGa-2 than onto KGa-1. The value of α_1 was higher for KGa-2 than for KGa-1 (Table 1), hence there was higher affinity of bacteria for KGa-2 than for KGa-1 [1,33]. In addition, Q° was

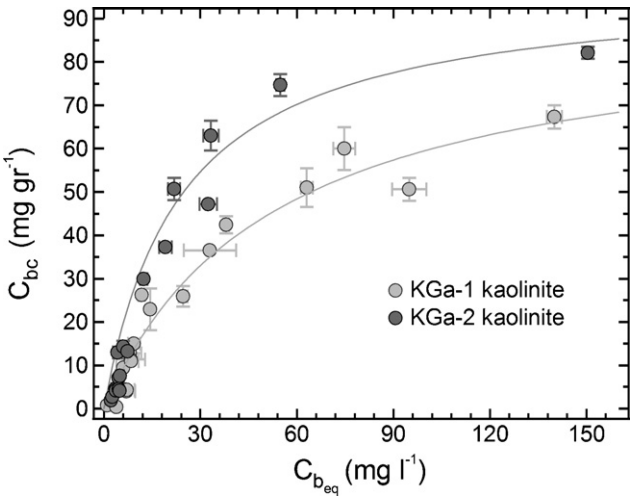

Fig. 1. Equilibrium attachment data of *P. putida* onto two differently structured kaolinite particles (symbols) and fitted Langmuir isotherm (curves).

Table 1
Fitted parameters obtained from the *P. putida* sorption experiments.

Kaolinite	Q° ((mg bacteria)(g clay)$^{-1}$)	α_1 ((l)(mg bacteria)$^{-1}$)	R
KGa-1	90.91	0.019	0.979
KGa-2	98.06	0.042	0.968

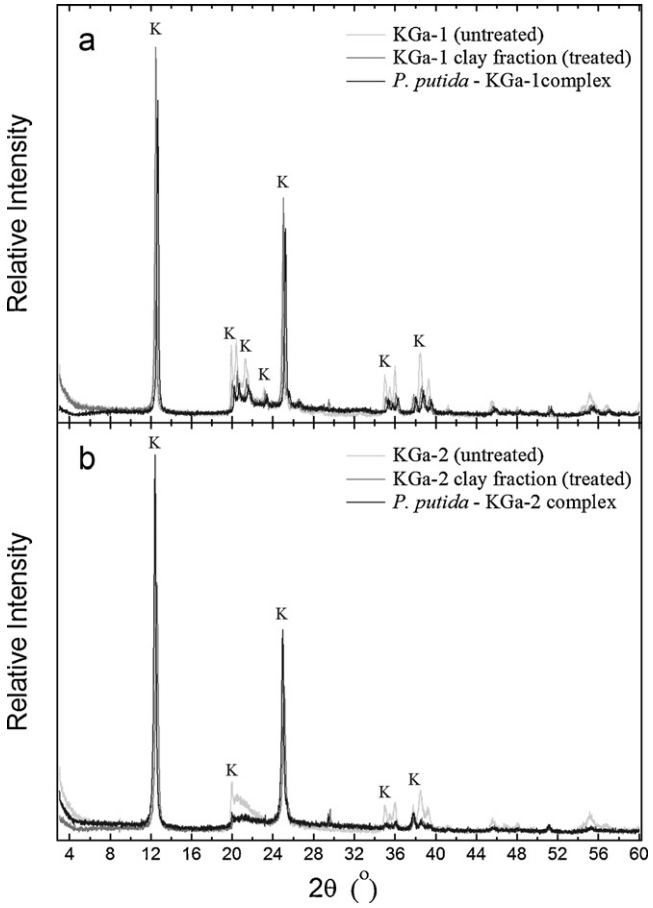

Fig. 2. X-ray diffraction patterns of (a) standard KGa-1 (untreated), KGa-1 clay fraction (treated) and *P. putida*–KGa-1 complex obtained from the batch experiment with bacterial concentration of 80 mg l^{-1}, and (b) KGa-2 (untreated), KGa-2 clay fraction (treated) and *P. putida*–KGa-2 complex obtained from the batch experiments with *P. putida* concentration of 80 mg l^{-1}.

greater for KGa-2 than for KGa-1, because KGa-2 has higher SSA and CEC. The SSA for KGa-1 was 10.05 $m^2\ g^{-1}$ and for KGa-2 was 23.50 $m^2\ g^{-1}$, while the CEC for KGa-1 was 2.0 mequiv./100 g and for KGa-2 was 3.3 mequiv./100 g. Typically, clay minerals with high SSA and CEC values are associated with high attachment capacity [1]. Note that other researchers have reported in the literature that there is no correlation between the amount of *P. putida* attached and the SSA of the clay [33,34].

The lower attachment of *P. putida* onto KGa-1 than onto KGa-2 was attributed to the higher Zeta potential of KGa-1 (−22.53 mV) compared to that of KGa-2 (−16.50 mV). The repulsive forces between negatively charged cells of *P. putida* and negatively charged kaolinite surfaces increase with increasing negative charge of the suspended particles. Thus, the experimental results of this study suggested that electrostatic forces play a vital role in the attachment of *P. putida* onto kaolinite. Other studies have also indicated that electrostatic forces affect the attachment of *P. putida* onto clay minerals [33] and goethite [41].

3.2. X-ray diffraction

The XRD patterns of KGa-1 and KGa-2 (standard samples, untreated), their clay fractions (treated), and bacteria–clay complexes obtained from the batch experiments, are presented in Fig. 2. It is evident from the XRD patterns that the clay fractions were enriched in kaolinite (higher d_{001} peaks at about $2\theta = 12.4^\circ$) and were characterized by the presence of the peaks of only one mineral (kaolinite). No new reflections were found on the bacteria–kaolinite complexes compared to those that appeared on the standard kaolinite samples.

3.3. ATR-FTIR

The ATR-FTIR spectra of ddH_2O, bacteria, KGa-1 and KGa-2 clay fractions and bacteria-kaolinite complexes are illustrated in Fig. 3. The main absorption bands of the bacteria were observed at: 1068 cm^{-1} due to the polysaccharide ring vibrations; 1400 cm^{-1}

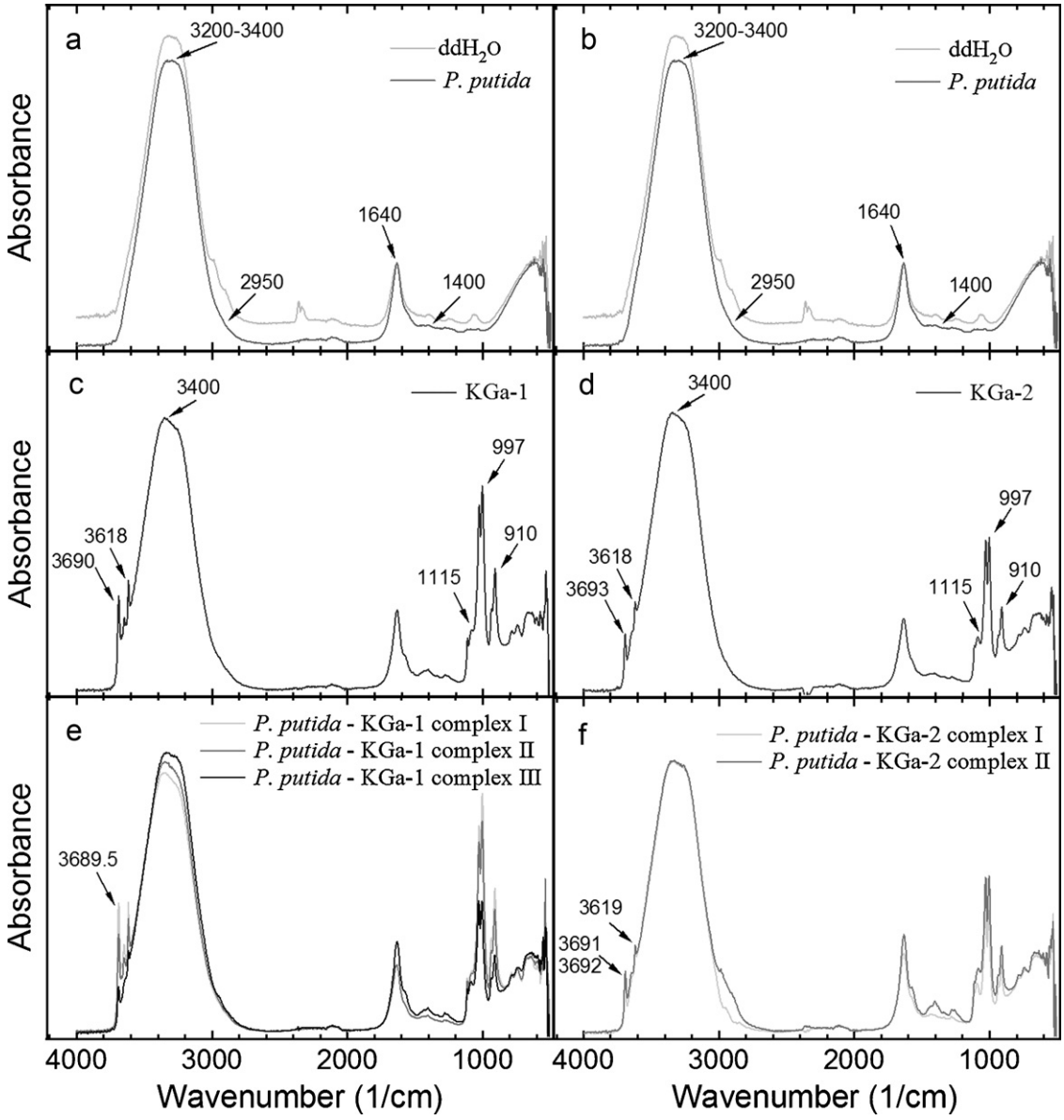

Fig. 3. ATR-FTIR spectra of (a) *P. putida* and ddH_2O, (b) *P. putida* and ddH_2O, (c) KGa-1 clay fraction, (d) KGa-2 clay fraction, and (e) *P. putida*–KGa-1 complex obtained from batch experiments with *P. putida* concentration of (I) 10 $mg\ l^{-1}$, (II) 50 $mg\ l^{-1}$ and (III) 160 $mg\ l^{-1}$, and (f) *P. putida*–KGa-2 complex obtained from batch experiments with *P. putida* concentration of (I) 10 $mg\ l^{-1}$ and (II) 50 $mg\ l^{-1}$.

caused by the C–O bending of the carboxylate ions; 1640 cm^{-1} due to the amide I (C=O) different conformation; and 2950 cm^{-1} related to the CH_2 asymmetric stretching vibration from fatty acid (Fig. 3a and b). A broad and strong band at about 3200 and 3400 cm^{-1} was the symmetric stretching vibration (ν1 mode) of water molecules. For both of the kaolinites considered in this study (Fig. 3c and d), the absorption band at about 910 cm^{-1} was assigned to the Si–O–Si bending vibration and the strong bands at 997, 1025 and 1115 cm^{-1} to the Si–O stretching vibrations.

The ν1 mode of the water molecules on the minerals appeared at 3400 cm^{-1} for kaolinite. The bending vibrations (ν2 mode) of the water molecules on KGa-1 gave absorption peaks at: 3618, 3650 and 3690 cm^{-1} (Fig. 3c), and on KGa-2 at: 3618, 3652 and 3693 cm^{-1} (Fig. 3d). No new absorption band was found for the bacteria–kaolinite complexes compared to those that appeared for the bacterial cells and kaolinite particles. However, the vibrations of water molecules sorbed onto kaolinite shifted from 3690 to 3689.5 cm^{-1} for the case of KGa-1 (Fig. 3e, see *P. putida*–KGa-1 complexes I, II, III) and from 3618 to 3619 and from 3693 to 3691 cm^{-1} for the case of KGa-2 after the attachment of bacteria (Fig. 3f, see *P. putida*–KGa-2 complex II). It should be noted that the latter band was shifted more for the *P. putida*–KGa-2 complex II than for the *P. putida*–KGa-2 complex I (appeared at 3692 cm^{-1}). These shifts suggested that the water molecules onto the clay minerals were involved in the attachment of *P. putida* onto both KGa-1 and KGa-2, and more intensively onto KGa-2.

The FTIR spectroscopy has been employed by various investigators for the assessment of the binding mechanism between adsorbates and minerals. Chen et al. [1] reported that the attachment of the pesticide carbaryl onto clay mineral surfaces resulted from hydrogen and electrovalent bonds; however, covalent bonds with some functional groups such as Si–O, Fe–OH may also be formed. Parikh and Chorover [42] used ATR-FTIR in order to investigate *Shewanella oneidensis*, *P. aeruginosa*, and *B. subtilis* attachment onto hematite. They suggested that phosphate/phosphonate and phosphodiester groups of bacteria were involved in the adhesion of bacteria. Jucker et al. [43] showed that the attachment of bacterial surface polysaccharides onto mineral oxides was mediated by hydrogen bonds.

The shifts in the vibration of water molecules observed in this study were related to the formation of hydrogen bonding between bacteria and minerals [34,44]. According to Rong et al. [34,41] hydrogen bonding was one of the governing factors in the attachment of *P. putida* onto kaolinite, montmorillonite and goethite.

3.4. NMR

NMR is an effective tool for the investigation of the structure and dynamic behaviour of water molecules near solid surfaces [45,46]. This is because both T_1 longitudinal (spin–lattice) and T_2 transverse (spin–spin) proton relaxation times are significantly reduced near a solid surface. In pure liquid water the molecular motions are rapid and random so that the ^1H T_1 and T_2 values are of the same order of magnitude and approximately equal to one second ($T_1 \approx T_2 \approx 1$ s). On the contrary, the ^1H relaxation times of water in heterogeneous systems differ greatly from those of pure water. These differences occur when water is confined in such heterogeneous media. The water molecules can experience: (1) strongly adsorbing sites such as hydroxyl groups, (2) the interface at the substrate material (e.g. presence of paramagnetic sites), and (3) relatively free conditions at some distance away from the substrate material.

Kaolinite belongs to the family of layer lattice silicates where the layers do not expand in water. In the *P. putida*–kaolinite system, a portion of the water and bacteria molecules were adsorbed on the delaminated layers of kaolinite and another portion of the molecules could be associated with molecules relatively away from the clay surface layers. Therefore, water can be considered to be in two different 'environments' or phases, an adsorbed phase and a more free one, each characterized by a specific nuclear T_1 spin–lattice relaxation time. The water molecules not only occupy the various environments, but they also migrate among them by means of translational diffusion. The motions that affect the relaxation times must include this exchange.

If there is no exchange of water molecules between these two phases or if this exchange is slow compared to the relaxation phase in the two phases, so that $C_i \ll T_{1,i}^{-1}$ (where C_i is the probability per unit time that a spin in the ith phase leaves this phase), the longitudinal relaxation function, $F(t)$, of the spin magnetization becomes the sum of two exponential terms decaying with the relaxation rates $T_{1,a}^{-1}$ and $T_{1,b}^{-1}$ as follows:

$$F(t) = \frac{N_a}{N}\exp\left[\frac{-t}{T_{1,a}}\right] + \frac{N_b}{N}\exp\left[\frac{-t}{T_{1,b}}\right] \quad (2)$$

where N_a and N_b are the number of spins in the two phases a and b, and $N = N_a + N_b$. However, if the exchange is rapid, so that $C_i \gg T_{1,i}^{-1}$, $F(t)$ becomes a simple exponential function:

$$F(t) = \exp\left[\frac{-t}{T_{1,\text{eff}}}\right] \quad (3)$$

which is decaying with an average relaxation rate:

$$\frac{1}{T_{1,\text{eff}}} = \frac{N_a}{N}\frac{1}{T_{1,a}} + \frac{N_b}{N}\frac{1}{T_{1,b}} \quad (4)$$

The intermediate case has been treated analytically by Zimmerman and Brittin [47].

Fig. 4 shows the T_1 distribution profiles, obtained by inverse Laplace transformation of the experimental T_1 relaxation data. In all samples the amount of KGa-1 and KGa-2 remained constant while the initial concentration of *P. putida* was different in each sample. It is evident from Fig. 4 that the inverse Laplace transform

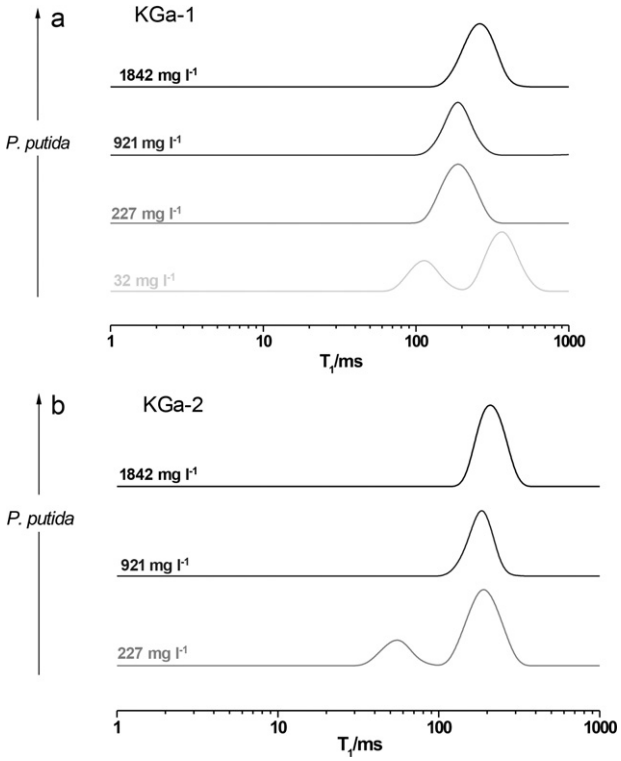

Fig. 4. T_1 distribution profiles of *P. putida* attached onto (a) KGa-1 and (b) KGa-2, for various initial *P. putida* concentrations.

gave a single or a double peak, as suggested by the expressions (3) and (2), respectively. Furthermore, the case of high initial *P. putida* concentration was described by a single T_1 relaxation time (single peak at around 200 ms), indicating a fast or intermediate exchange. On the contrary, for the case of low initial *P. putida* concentration (32 and 227 mg l^{-1} for KGa-1 and KGa-2, respectively), two well-isolated phases (double peak) were clearly observed, indicating a slow exchange between the two phases (adsorbed and free). It is important to note that the slow exchange two-phase model is more representative of the KGa-2 with the higher initial *P. putida* concentration (227 mg l^{-1}) than the KGa-1 (32 mg l^{-1}). This means that KGa-2 can accommodate more *P. putida* than KGa-1 and still can be characterized by the slow exchange model. This observation was in accordance with the macroscopic results (sorption isotherms) and clearly indicated that KGa-2 has a larger attachment capacity than KGa-1. This may be ascribed to the disordered nature of KGa-2 layers. Thus, NMR offered a microscopic confirmation of the fact that the amount of *P. putida* attached onto kaolinite was higher in the poorly crystalline sample KGa-2 than in the highly crystalline sample KGa-1.

4. Conclusions

The experimental results presented herein indicated that the attachment of *P. putida* onto pure kaolinite could be described by a Langmuir type isotherm. It was observed that more *P. putida* attached onto poorly crystallized kaolinite (KGa-2) than onto well-crystallized kaolinite (KGa-1). Electrostatic interactions and hydrogen bonding were considered to play a significant role in the adhesion of bacteria onto clay minerals. The higher SSA value of KGa-2 indicated that *P. putida* exhibited stronger hydrogen bonding with KGa-2 than KGa-1. Finally, the NMR spectroscopic technique distinguished the different attachment capacities of KGa-1 and KGa-2.

References

[1] H. Chen, X. He, X. Rong, W. Chen, P. Cai, W. Liang, S. Li, Q. Huang, Appl. Clay Sci. 46 (2009) 102.
[2] F. Compere, G. Porel, F. Delay, J. Contam. Hydrol. 49 (2001) 1.
[3] S.S. Gupta, K.G. Bhattacharyya, J. Colloid Interface Sci. 295 (2006) 21.
[4] E. Alvarez-Ayuso, A. Garcia-Sanchez, Clays Clay Miner. 51 (2003) 475.
[5] Y. Sim, C.V. Chrysikopoulos, Colloids Surf. A: Physicochem. Eng. Aspects 155 (1999) 189.
[6] V.I. Syngouna, C.V. Chrysikopoulos, Environ. Sci. Technol. 44 (2010) 4539.
[7] A. Torrents, S. Jayasundera, Chemosphere 35 (1997) 1549.
[8] L.S. Hundal, M.L. Thompson, D. Laird, M. Carmo, Environ. Sci. Technol. 35 (2001) 3456.
[9] R. Anders, C.V. Chrysikopoulos, Water Resour. Res. 41 (2005) W10415, doi:10.1029/2004WR003419.
[10] R. Anders, C.V. Chrysikopoulos, Transp. Porous Media 76 (2009) 121.
[11] C. Masciopinto, R. La Mantia, C.V. Chrysikopoulos, Water Resour. Res. 44 (2008) W01404, doi:10.1029/2006WR005643.
[12] C.V. Chrysikopoulos, Y. Sim, J. Hydrol. 185 (1996) 199.
[13] Y. Sim, C.V. Chrysikopoulos, Transp. Porous Media 30 (1998) 87.
[14] P. Nannipieri, J. Ascher, M.T. Ceccherini, L. Landi, G. Pietramellara, G. Renella, Eur. J. Soil Sci. 54 (2005) 655.
[15] C.V. Chrysikopoulos, C. Masciopinto, R. La Mantia, I.D. Manariotis, Environ. Sci. Technol. 44 (2010) 971.
[16] A. Abdel-Salam, C.V. Chrysikopoulos, Transp. Porous Media 20 (1995) 197.
[17] H.M. Bekhit, A.E. Hassan, Water Resour. Res. 43 (2007) W08409, doi:10.1029/2006WR005418.
[18] N.K. Dhand, J.L.M.L. Toribio, R.J. Whittington, Appl. Environ. Microbiol. 75 (2009) 5581.
[19] H.M. Bekhit, M.A. El-Kordy, A.E. Hassan, J. Contam. Hydrol. 108 (2009) 152.
[20] A.K. Guber, D.R. Shelton, Y.A. Pachepsky, J. Environ. Qual. 34 (2005) 2086.
[21] J.W.A. Foppen, J.F. Schijven, Water Res. 39 (2005) 3082.
[22] S.B. Kim, S.J. Park, C.G. Lee, N.C. Choi, D.J. Kim, Colloids Surf. B: Biointerfaces 63 (2008) 236.
[23] C.F. Leon-Morales, A.P. Leis, M. Strathmann, H.C. Flemming, Water Res. 38 (2004) 3614.
[24] I.A. Vasiliadou, C.V. Chrysikopoulos, Water Resour. Res. 47 (2011) W02543, doi:10.1029/2010WR009560.
[25] X. Rong, Q. Huang, W. Chen, Appl. Clay Sci. 38 (2007) 97.
[26] E. Courvoisier, S. Dukan, Appl. Clay Sci. 44 (2009) 67.
[27] L.N. Warr, J.N. Perdrial, M.C. Lett, A. Heinrich-Salmeron, M. Khodja, Appl. Clay Sci. 46 (2009) 337.
[28] S.K. Chaerun, K. Tazaki, Clay Miner. 40 (2005) 481.
[29] J.E. Kostka, D.D. Dalton, H. Skelton, S. Dollhopf, J.W. Stucki, Appl. Environ. Microbiol. 68 (2002) 6256.
[30] S. Hwang, R.L. Tate III, Biol. Fertil. Soils 24 (1997) 335.
[31] N. Yee, J.B. Fein, C.J. Daughney, Geochim. Cosmochim. Acta 64 (2000) 609.
[32] A.R. Shashikala, A.M. Raichur, Colloids Surf. B: Biointerfaces 24 (2002) 11.
[33] D. Jiang, Q. Huang, P. Cai, X. Rong, W. Chen, Colloid Surf. B: Biointerfaces 54 (2007) 217.
[34] X. Rong, Q. Huang, X. He, H. Chen, P. Cai, W. Liang, Colloids Surf. B: Biointerfaces 64 (2008) 49.
[35] D. Grasso, B.F. Smets, K.A. Strevett, B.D. Machinist, Environ. Sci. Technol. 30 (1996) 3604.
[36] D. Ams, J. Fein, H. Dong, P. Maurice, Geomicrobiol. J. 21 (2004) 511.
[37] D. Rickwood, T. Ford, J. Graham, Anal. Biochem. 123 (1982) 23.
[38] E. Karakosta, G. Diamantopoulos, M.S. Katsiotis, M. Fardis, G. Papavassiliou, P. Pipilikaki, M. Protopapas, D. Panagiotaras, Ind. Eng. Chem. Res. 49 (2010) 613.
[39] E. Laganas, G. Papavassiliou, M. Fardis, A. Leventis, F. Milia, E. Chaniotakis, C. Meletiou, J. Appl. Phys. 77 (1995) 3343.
[40] S.W. Provencher, Comput. Phys. Commun. 27 (1982) 213.
[41] X. Rong, W. Chen, Q. Huang, P. Cai, W. Liang, Colloids Surf. B: Biointerfaces 80 (2010) 79.
[42] S.J. Parikh, J. Chorover, Langmuir 22 (2006) 8492.
[43] B.A. Jucker, H. Harms, S.J. Hug, A.J.B. Zehnder, Colloids Surf. B: Biointerfaces 9 (1997) 331.
[44] D. Santhiya, S. Subramanian, K.A. Natarajan, J. Colloid Interface Sci. 235 (2001) 289.
[45] J. Fripiat, J. Cases, M. Francois, M. Letellier, J. Colloid Interface Sci. 89 (1982) 378.
[46] H. Winkler, D. Michel, Adv. Colloid Interface Sci. 23 (1985) 149.
[47] J.R. Zimmerman, W.E. Brittin, J. Chem. Phys. 61 (1957) 1328.